



Synthesis and photoluminescent properties of four novel trinuclear europium complexes based on two tris- β -diketones ligands

Chaolong Yang^{a,b}, Jianxin Luo^{a,b}, Jianying Ma^{a,b}, Mangeng Lu^{a,*}, Liyan Liang^a, Bihai Tong^c

^aGuangzhou Institute of Chemistry, Chinese Academy of Sciences, Guangzhou 510650, PR China

^bGraduate School of the Chinese Academy of Sciences, Beijing 100039, PR China

^cAnhui Univ Technol, Inst Mol Engrn & Appl Chem, Coll Met & Resources, Maanshan, Anhui 243002, PR China

ARTICLE INFO

Article history:

Received 4 May 2011

Received in revised form

16 June 2011

Accepted 16 June 2011

Available online 29 June 2011

Keywords:

Photoluminescence

Trinuclear europium complex

Quantum yield

Tris- β -diketones

Luminescent lifetime

OLEDs

ABSTRACT

Four novel trinuclear europium complexes with two tris- β -diketones ligands have been synthesized, and the chemical structures of ligands and complexes were characterized by FT-IR, UV–vis, ¹H NMR, ¹³C NMR, XRD, ESI-MS, and element analysis. The photoluminescent properties of trinuclear complexes in solid and THF solution were investigated. All trinuclear complexes exhibited strong relative luminescent intensity and long luminescent lifetime. Meanwhile, the results of lifetime decay curves indicated that only one chemical environment existed around the europium ion. The intrinsic luminescent quantum yields (Φ_{LN}) and experimental intensity parameters of trinuclear complexes were obtained based on the emission spectra and luminescent lifetime of ³D₀ excited state for europium ion. All trinuclear europium complexes exhibited relative high intrinsic luminescent yield and intensity parameters. Especially, due to the contribution of addition two europium lumophors in trinuclear europium complexes, the trinuclear complexes containing TTA exhibited much longer lifetime and higher intrinsic quantum yield than mononuclear europium complex Eu(TTA)₃phen.

© 2011 Elsevier Ltd. All rights reserved.

1. Introduction

As one of the most promising next generation low cost full color flat panel displays, organic light-emitting diodes (OLEDs) have attracted much research interest since of Tang and Van Slyke pioneering work in 1987 [1]. For commercial application, three primary colors of blue [2,3], green, and red are basically required. Until now, pure red luminescent material is still a challenge, although many transition metal complexes showing red emission have been reported [4–6]. Among those red light-emitting materials, europium complexes are particular and attractive, because they can emit highly monochromatic red light at around 612 nm with half peak bandwidths of 5–10 nm due to the electronic transitions of the central europium ion. In addition, they can offer 100% emission intrinsic quantum efficiency theoretically since this kind of transition is not restricted by the spin inhibition rule [7]. Such characteristics originate from the inner 4f electrons which are shielded from their outer filled 5s and 5p shells. Unfortunately, the long luminescent lifetimes of europium ion result in a low absorption coefficient. To overcome the problem, organic ligands

which have much large absorption coefficient are usually coordinated to sensitize europium complexes. So the design and synthesis of organic ligands with larger absorption coefficient are very important to improve the europium complexes luminescent properties. Recently, many organic ligands with larger absorption coefficient have been designed and synthesized.

One efficient approach to increase the luminescent properties is to introduce ligands with multiple binding sites [8–10]. So far, the organic europium complexes have been studied for twenty years. However, the great majority of europium complexes studied is mononuclear and binuclear complexes [11–14]. There are few reports of the synthesis and properties for trinuclear europium complexes [15].

We have been interested in studying luminescent properties for tris(8-quinolinolato)aluminum complexes and lanthanide complexes [16], and have recently used tris- β -diketonates as sensitizers for lanthanide luminescence [17], the result indicated that one tris- β -diketones can coordinated three lanthanide ions and improve the lanthanide complexes luminescent properties. Our previous work and some reported results [8,17–19] showed that the luminescent properties of dinuclear and trinuclear lanthanide complexes were higher than mononuclear ones, and the lifetimes of dinuclear and trinuclear complex were longer than mononuclear ones.

* Corresponding author. Tel./fax: +86 20 85232978.

E-mail address: mglu@gic.ac.cn (M. Lu).

In this paper, to further improve the luminescent properties of europium complexes, four novel trinuclear europium complexes based on two tris- β -diketones ligands were designed and synthesized. The structures of the ligands and trinuclear europium complexes were characterized by FT-IR, UV-vis, ^1H NMR, ^{13}C NMR, ESI-MS, element analysis. The photoluminescent properties and thermal stability were investigated by photoluminescent (PL) spectroscopy and thermogravimetric analysis (TGA), respectively. For all trinuclear europium complexes, every tris- β -diketones ligand contains three β -diketones, and can coordinate with three europium ions. We expect that these trinuclear complexes can exhibit excellent luminescent properties.

2. Experimental section

2.1. Materials and measurements

Starting materials were of reagent grade and used without further purification, unless otherwise stated. All solvents were purified with conventional methods before used. Mesitylene, Dibenzoylmethane (DBM), potassium tert-butoxide, 2-thenoyltrifluoroacetone (TTA), and phenanthroline were purchased from Aldrich Chemical Company. Eu_2O_3 (99.99%) was purchased from a Chinese company, Beijing Founder. $\text{EuCl}_3 \cdot 6\text{H}_2\text{O}$ ethanol solution was obtained by dissolving Eu_2O_3 in concentrated chlorhydric acid.

Melting points were determined on SGW X-4 micro-melting point apparatus (Shanghai PSE Co. Ltd). Elemental analysis data were obtained from Vario EL elemental analyzer. NMR spectra were taken on a DRX-400 MHz (Bruker) superconducting-magnet NMR spectrometer with TMS as an internal standard. FT-IR spectra were carried out using an RFX-65A (Analects) Fourier Transform Infrared Spectrometer. Thermogravimetric analysis (TGA) was performed with Pyris 1 TGA instrument at a heating rate of $10^\circ\text{C}/\text{min}$ under nitrogen atmosphere. UV-vis absorption spectrum was determined on a Shimadzu spectrophotometer. The photoluminescence (PL) measurements in solid state and THF solution were conducted in a Hitachi F-4600 fluorescence spectrophotometer. Luminescence lifetimes were obtained with the PLSP20 steady state spectrometer with a pulsed xenon lamp. X-ray diffraction (XRD) measurements were carried out with a Rigaku Diffractometer (D/MAX-12000).

2.2. Synthesis of 1,3,5-tris(bromomethyl)-2,4,6-trimethylbenzene

1,3,5-tris(bromomethyl)-2,4,6-trimethylbenzene was prepared according to the procedure described in the literature with some modification [20]. Mesitylene (12 g, 100 mmol), paraformaldehyde (10.26 g, 340 mmol) and 75 ml of glacial acetic acid was rapidly added to a 150 ml three neck round bottom flask with 75 ml of HBr/acetic acid solution during magic stirring. The mixture solution was heated to 95°C and kept at this temperature for 8 h, then poured into 200 ml of water to give amounts of white solid. The product from filtering was washed with 200 ml of anhydrous ethanol, and then was filtered and dried overnight at 60°C to give 33.5 g of title compound, yield 85%, mp $183\text{--}186^\circ\text{C}$. FT-IR (KBr) (cm^{-1}): 785, 1446.1, 2922. ^1H NMR (400 MHz, CDCl_3): δ 2.44 (s, 9H, Ar- CH_3), 4.56 (s, 6H, - CH_2Br). ^{13}C NMR (100 MHz, CDCl_3): δ 12.1, 27.5, 134.7, 137.1.

2.3. Synthesis of 1,3,5-tris(bromomethanyl)benzene

Mesitylene (10.12 g, 84 mmol), NBS (45.30 g, 255 mmol) and AIBN (45.9 mg) were heated to reflux at 90°C in 120 ml of dry CCl_4 under N_2 with stirring for 40 h. The solution was then cooled in an ice bath and the succinimide was filtered off and washed with carbon tetrachloride. The filtrate was washed by saturated sodium hydrogen carbonate solution and water, and then dried with

anhydrous Na_2SO_4 . The volume was reduced to approximately 50 ml and then light petroleum (100 ml) was added. The solution was placed in freezer and the resulting oily solid was filtered off. This progress was repeated several times and the crops of oily solid were combined. The product was then recrystallized from light petroleum to yield 1,3,5-tris(bromomethyl)benzene as colorless needles, yield 40% (1.5 g), mp $87\text{--}89^\circ\text{C}$. ^1H NMR (400 MHz, CDCl_3): δ 4.44 (s, 6H, - CH_2Br), 7.34 (s, 3H, ArH). Anal. Calcd. for $\text{C}_9\text{H}_9\text{Br}_3$: C, 30.29; H, 2.54; Found: C, 30.51; H, 2.37.

2.4. General procedure of synthesis of tris- β -diketones

Tris- β -diketones were synthesized according to that discussed in reference [21]. Dibenzoylmethane (30 mmol) was added to a refluxing solution of tert-butanol (250 ml) and potassium tert-butoxide (20 mmol). 10 mmol of 1,3,5-tris(bromomethyl)-2,4,6-trimethylbenzene or 1,3,5-tris(bromomethanyl)benzene was then added in some portions followed by a catalytic amount of potassium iodide. The mixture solution was kept at reflux temperature for 48 h, then tert-butanol was removed under reduced pressure, the residue product was separated by dichloromethane (150 ml) and water (100 ml), organic phase was dried over anhydrous sodium sulfate. Some pale-yellow oil was given when dichloromethane was removed in vacuum, the oil was solidified for two days to get pale-yellow solid. This was recrystallized from ethyl acetate to give colorless crystalline.

1,3,5-Tris(3'-methyl-2', 4'-pentanedione)-2,4,6-trimethylbenzene (H_3L^1) was synthesized in a yield 72% (5.9 g), mp $207\text{--}209^\circ\text{C}$. ^1H NMR (400 MHz, CDCl_3): δ 7.24–7.69 (30H, m, Ph), 5.01 (3H, t, COCHCO), 3.40 (6H, d, CH_2), 1.90 (9H, s, CH_3). ^{13}C NMR (100 MHz, CDCl_3): δ 17.2 (CH_3), 30.2 (CH_2), 58.2 (CH), 128.6 (CH), 128.7 (C), 133.5 (CH), 133.8 (CH), 134.9 (C), 135.9 (C), 196.2 (C=O). (Found: C, 82.49; H, 5.96; $\text{C}_{57}\text{H}_{48}\text{O}_6$ requires C, 82.57; H, 5.84) FT-IR (KBr): ν (C=O) 1693, 1660 cm^{-1} . ESI-MS (m/z): 851 ($M + \text{Na}^+$).

1,3,5-Tris(2,2-dibenzoyl ethyl) benzene (H_3L^2) was prepared in a yield 65% (5.1 g), mp $87\text{--}89^\circ\text{C}$. ^1H NMR (400 MHz, CDCl_3): δ 16.88 (s, 3H, -OH) 7.97–7.99 (d, 12H, Ph) 7.52–7.56 (t, 6H, Ph) 7.46–7.50 (t, 12H, Ph), 6.85 (s, 3H, Ph), 3.41 (s, 6H, - CH_2). ^{13}C NMR (100 MHz, CDCl_3): δ 34.8 (CH_2), 58.5 (CH), 128.5 (CH), 128.8 (CH), 133.5 (CH), 135.8 (C), 139.9 (C), 195.4 (C=O). (Found: C, 81.73; H, 5.87; $\text{C}_{54}\text{H}_{42}\text{O}_6$ requires C, 82.42; H, 5.38) FT-IR (KBr): ν (C=O) 1697, 1670 cm^{-1} . ESI-MS (m/z): 810 ($M + \text{Na}^+$).

2.5. General procedure of synthesis of trinuclear Eu-complexes

Ligand H_3L^1 or H_3L^2 (0.5 mmol), Phen. H_2O (1.5 mmol) and 0.2 g potassium tert-butoxide were dissolved in 50 ml anhydrous ethanol, then the solution was heated to 60°C , 20 ml anhydrous ethanol with $\text{EuCl}_3 \cdot 6\text{H}_2\text{O}$ (1.5 mmol) was gradually added to the solution. After 1 h, corresponding β -diketone (3 mmol) was added to the mixed solution and reacted at this temperature for another 10 h, mixed solution was cooled to room temperature and removed solvents, residual solid was dissolved by 50 ml chloroform, and washed three times with 80 ml water every time, then removed chloroform through reduced pressure to give the desired trinuclear europium complexes.

$\text{Eu}_3(\text{DBM})_3(\text{phen})_3\text{H}_2\text{O}^1$ was prepared in a yield 70% as light-yellow powder. ^1H NMR (400 MHz, CDCl_3): δ , ppm 10.96 (br s, Phen-H), 10.58 (br s, Phen-H), 9.94 (br s, Ph-H), 8.93 (br s, Ph-H), 7.98–8.13 (br d, Ph-H), 7.24–7.48 (br d, Ph-H), 6.49–6.70 (br d, Ph-H), 5.84 (br s, Ph-H), 4.71 (br s, COCHCO), 3.13 (br s, - CH_2), 2.72 (br s, H_2O), 2.32 (br s, - CH_3). (Found: C, 63.92; H, 4.15; N, 3.01. $\text{Eu}_3\text{C}_{138}\text{H}_{114}\text{N}_6\text{O}_{18}$ requires C, 63.74; H, 4.42; N, 3.23) FT-IR (KBr): ν (C=O) 1596, 1551 cm^{-1} , (C=C) 1518 cm^{-1} , (Eu \rightarrow O) 515 cm^{-1} , (Eu \rightarrow N) 422 cm^{-1} .

$\text{Eu}_3(\text{DBM})_6(\text{phen})_3\text{L}^2$ was prepared in a yield 75% as light-yellow powder. ^1H NMR (400 MHz, CDCl_3): δ , ppm 10.99(br s, Ph–H), 10.59(br s, Ph–H), 10.01(br s, Ph–H), 8.96(br s, Ph–H), 7.96(br s, Ph–H), 7.48–7.52(br d, Ph–H), 7.24(br s, Ph–H), 6.72(br s, Ph–H), 6.03(br s, Ph–H), 4.82(br s, COCHCO), 3.26(br s, $-\text{CH}_2$). (Found: C, 68.9; H, 4.15; N, 2.83; $\text{Eu}_3\text{C}_{180}\text{H}_{129}\text{N}_6\text{O}_{18}$ requires C, 69.30; H, 4.17; N, 2.69.) FT-IR(KBr): ν ($\text{C}=\text{O}$) 1597, 1550 cm^{-1} , ($\text{C}=\text{C}$) 1518 cm^{-1} , ($\text{Eu}\rightarrow\text{O}$) 515 cm^{-1} , ($\text{Eu}\rightarrow\text{N}$) 422 cm^{-1} .

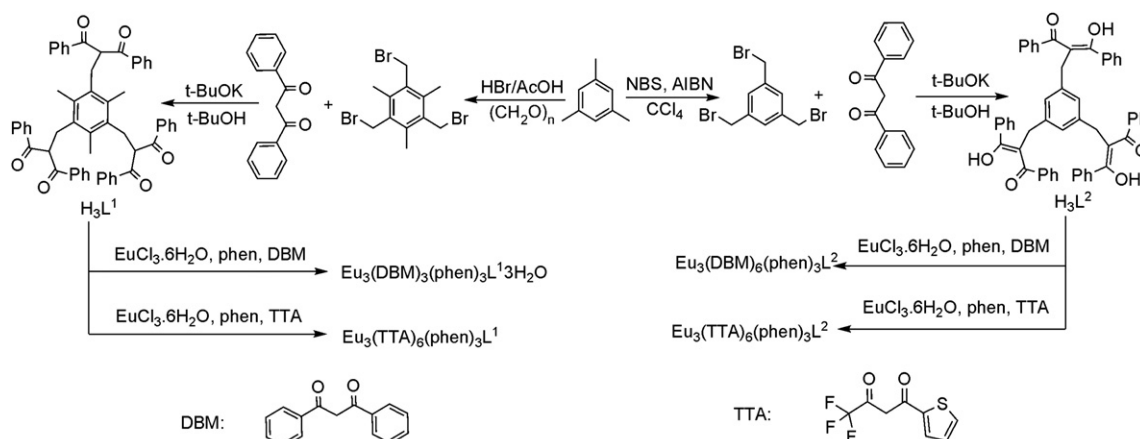
$\text{Eu}_3(\text{TTA})_6(\text{phen})_3\text{L}^1$ was prepared in a yield 65% as milk-white powder. ^1H NMR (400 MHz, CDCl_3): δ , ppm 10.19(br s, phen-H), 9.52(br s, $-\text{phen}$ and Ph–H), 8.48(br s, Ph–H and Th–H), 8.14(br s, Ph–H), 7.45(br d, Ph–H), 6.93(br s, Th–H and phen–H), 6.27–6.46(br d, Th–H and Ph–H), 4.43(br s, COCHCO), 3.04(br s, $-\text{CH}_2$), 2.34(br s, $-\text{CH}_3$). (Found: C, 53.39; H, 3.05; N, 2.81; $\text{Eu}_3\text{C}_{141}\text{H}_{96}\text{F}_{18}\text{N}_6\text{O}_{18}\text{S}_6$ requires C, 53.77; H, 2.98; N, 2.67.) FT-IR(KBr): ν ($\text{C}=\text{O}$) 1601, 1539 cm^{-1} , ($\text{C}=\text{C}$) 1512 cm^{-1} , ($\text{Eu}\rightarrow\text{O}$) 460 cm^{-1} , ($\text{Eu}\rightarrow\text{N}$) 418 cm^{-1} .

$\text{Eu}_3(\text{TTA})_6(\text{phen})_3\text{L}^2$ was prepared in a yield 77% as milk-white powder. ^1H NMR (400 MHz, $\text{DMSO}-d_6$): δ , ppm 9.09(br s, phen–H), 8.49(br s, $-\text{phen}$ and Ph–H), 7.95–7.99(br s, Ph–H and Th–H), 7.77(br s, Ph–H), 7.44(br d, Ph–H), 6.48(br s, Th–H and phen–H), 6.3(br s, Th–H and Ph–H), 4.51(br s, COCHCO), 3.68(br s, $-\text{CH}_2$). (Found: C, 51.61; H, 2.68; N, 2.97. $\text{Eu}_3\text{C}_{138}\text{H}_{87}\text{N}_6\text{F}_{18}\text{O}_{18}\text{S}_6$ requires C, 53.34; H, 2.82; N, 2.70.) FT-IR(KBr): ν ($\text{C}=\text{O}$) 1596, 1539 cm^{-1} , ($\text{C}=\text{C}$) 1509 cm^{-1} , ($\text{Eu}\rightarrow\text{O}$) 461 cm^{-1} , ($\text{Eu}\rightarrow\text{N}$) 418 cm^{-1} .

3. Results and discussion

3.1. Design and synthesis of ligands and trinuclear europium complexes

Synthetic routes for the ligands and europium complexes are outlined in Scheme 1. The H_3L^1 and H_3L^2 ligands were readily prepared in high yield (>65%) from the corresponding tri(bromomethyl) benzene and dibenzoylmethane (DBM) by refluxing in tert-butanol in the presence of t-BuOK. The resulting tris- β -diketones were readily purified by crystallization from acetic ester, and the ^1H NMR and ^{13}C NMR spectra are in accord with the presence of high levels of symmetry. The ligand H_3L^1 exists only one single tautomer, the diketone form, was observed by both ^1H and ^{13}C NMR spectra in deuteriochloroform. However, for ligand H_3L^2 , the enol tautomer was observed by ^1H and ^{13}C NMR spectra.



Scheme 1. Synthetic routes for ligands and trinuclear europium complexes.

Europium complexes are commonly synthesized by dissolving ligands in warm ethanol, neutralized pH = 7 with dilute sodium hydroxide solution, followed by the addition of the europium chloride solution. We attempted to prepare trinuclear europium complexes by the commonly procedure of heating with europium chloride and the corresponding β -diketones ligand in the presence of NaOH. Unfortunately, we failed. This because of the tris- β -diketones was decomposed in the presence of NaOH. In order to prepare trinuclear europium complexes, we used t-BuOK instead of NaOH as base, because the tris- β -diketones can not reaction with t-BuOK. The structures of trinuclear europium complexes were shown in Fig. 1.

Some reports showed that introducing ligands with multiple binding sites to lanthanide complexes can increase the luminescent properties of lanthanide complexes [8,17–19]. Recently, the great majority of europium complexes studied was mononuclear and binuclear complexes. There were few reports of the synthesis and properties for trinuclear europium complexes. So we designed and synthesized two tris- β -diketones ligands, every tris- β -diketones ligand can chelate three europium ions, and prepared four novel trinuclear europium complexes using tris- β -diketones as ligands. We attempted these trinuclear europium complexes can enhance the luminescent properties. Meanwhile, as well-known, the presence of C–H oscillators in the molecules can efficiently quench the luminescence of emitting center europium ion. Due to H_3L^1 ligand containing three methyl groups in center benzene ring, we presumed the luminescent properties of trinuclear europium complexes based on ligand H_3L^1 could be weaker than trinuclear europium complexes based on H_3L^2 under the same conditions.

3.2. FT-IR analysis

The FT-IR spectra of the ligands and corresponding europium complexes were shown in Fig. 2. The FT-IR spectra of trinuclear europium complexes based on DBM (or TTA) as another β -diketone ligand were analogical because the ligands H_3L^1 and H_3L^2 were similar. For these europium complexes based on DBM as another β -diketone ligand, the characteristic stretching vibration absorption peaks of $-\text{C}=\text{O}$ in H_3L^1 (or H_3L^2) and DBM shifted from ca. 1697 cm^{-1} to 1601 cm^{-1} , and a new absorption peak was observed at 1550 cm^{-1} , which attributed to $-\text{C}=\text{C}$ stretching vibration of H_3L^1 (H_3L^2) and DBM coordinated to with europium ion. The results suggested that the coordination bonds were formed between the H_3L^1 (H_3L^2) and europium ion. The ring vibration of 1, 10-phenanthroline was observed at 1517 cm^{-1} , although the

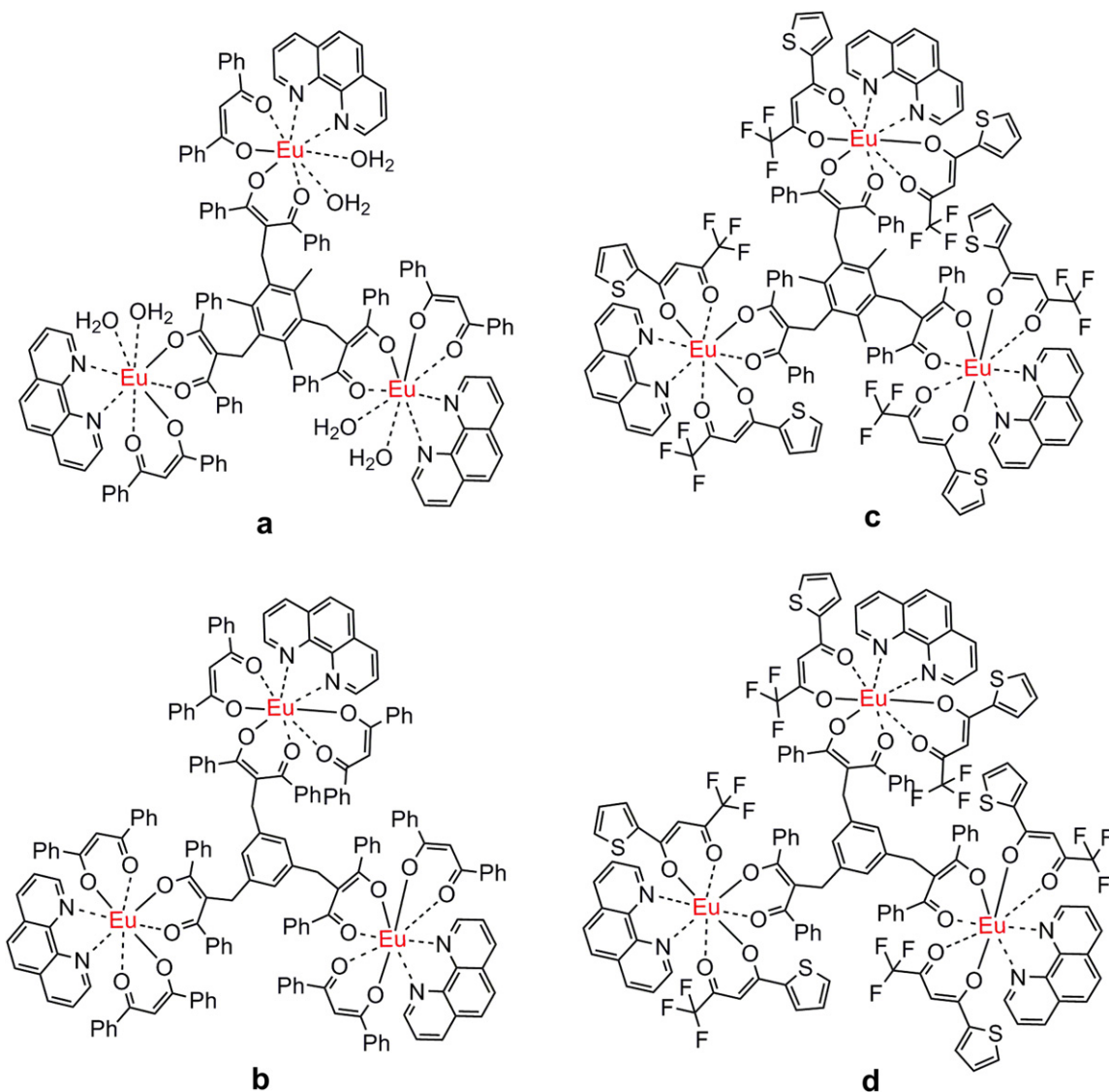


Fig. 1. The structures of trinuclear europium complexes based on tris- β -diketones as ligand, (a) $\text{Eu}_3(\text{DBM})_3(\text{phen})_3 \cdot 3\text{H}_2\text{O} \cdot \text{L}^1$, (b) $\text{Eu}_3(\text{DBM})_6(\text{phen})_3 \cdot \text{L}^2$, (c) $\text{Eu}_3(\text{TTA})_6(\text{phen})_3 \cdot \text{L}^1$, (d) $\text{Eu}_3(\text{TTA})_6(\text{phen})_3 \cdot \text{L}^2$.

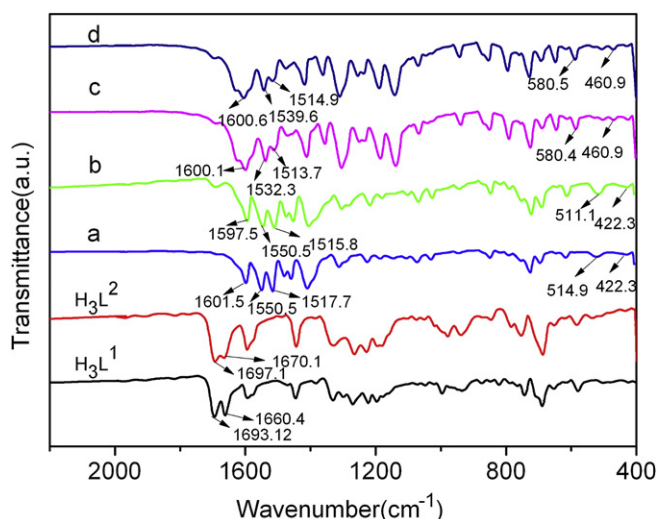


Fig. 2. FT-IR spectra of ligands and trinuclear europium complexes.

intensity was relatively weaker. Meanwhile, two new absorption peaks were observed at ca. 514 cm^{-1} and 422 cm^{-1} , they were attributed the stretching of $\text{O} \rightarrow \text{Eu}$ and $\text{N} \rightarrow \text{Eu}$, respectively. For these europium complexes based on TTA as another β -diketone ligand, the typical asymmetric vibrations of the carbonyl group of TTA and H_3L^1 (H_3L^2) were observed at about 1600 cm^{-1} from the FT-IR Spectra of corresponding complexes, the bond at about 580 cm^{-1} revealed the presence of $\text{O} \rightarrow \text{Eu}$, which could not be observed in ligands. Meanwhile, the peaks of phen at 738 cm^{-1} and 852 cm^{-1} corresponding to the stretching vibration of C–H bonds shifted to 723 cm^{-1} and 845 cm^{-1} , respectively. These FT-IR results further confirmed the conformation of the trinuclear europium complexes.

3.3. ^1H NMR spectra analysis

The lanthanide-based complexes were known as shift reagents due to paramagnetism of the lanthanide ion. Therefore, the peaks of ligands in lanthanide complexes were different with free ligands. Here, we chosen the trinuclear europium complex of $\text{Eu}_3(\text{TTA})_6(\text{phen})_3 \cdot \text{L}^2$ as an example discussed the chemical shift in ^1H NMR spectrum. The ^1H

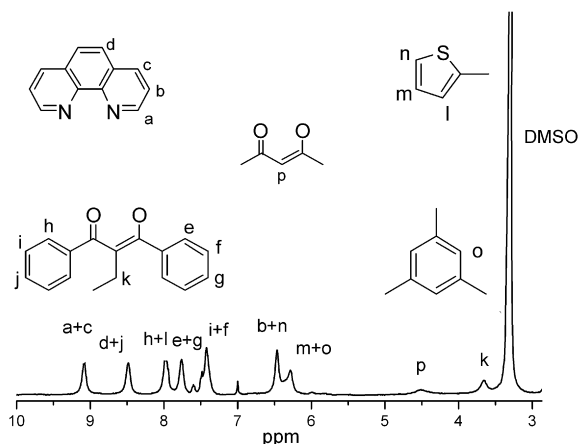


Fig. 3. ^1H NMR spectrum of trinuclear europium complex $\text{Eu}_3(\text{TTA})_6(\text{phen})_3\text{L}^2$.

NMR spectrum of the complex obtained at 400 MHz in *d*-DMSO solution was shown in Fig. 3. Although line broadening of certain peaks close to paramagnetic europium ion was observed, full assignments have been achieved using high resolution instruments to avoid signal overlap. The ^1H NMR spectrum of $\text{Eu}_3(\text{TTA})_6(\text{phen})_3\text{L}^2$ exhibited a broad singlet at 3.68 ppm, which integrated six protons and was assigned as proton of k position. The single peak at 4.51 ppm was attributable to the protons at the position (COCHCO) of the six TTAs. The peak at 6.30 ppm was attributed to the overlap of o and m position protons. Protons of b and n position appeared as a singlet peak at 6.48 ppm, with the expected integral value (12 H). A broad singlet at 7.44 ppm was assigned to the protons of i and f position for ligand H_3L^2 , which integrated 12 protons. The e and g position protons of phenyl for ligand H_3L^2 were observed at 7.77 ppm, which integrated 9 protons. The triplet peaks at 7.95–7.99 ppm were assigned to the protons of l position for TTAs and h position for ligand H_3L^2 . The protons of a, c position and d, j position were appeared at 9.09 ppm and 8.49 ppm, and which integrated 12 and 9 protons, respectively.

3.4. UV–vis analysis

The UV–vis absorption spectra for the ligands and trinuclear europium complexes in THF solution (1×10^{-5} mol/L) were shown

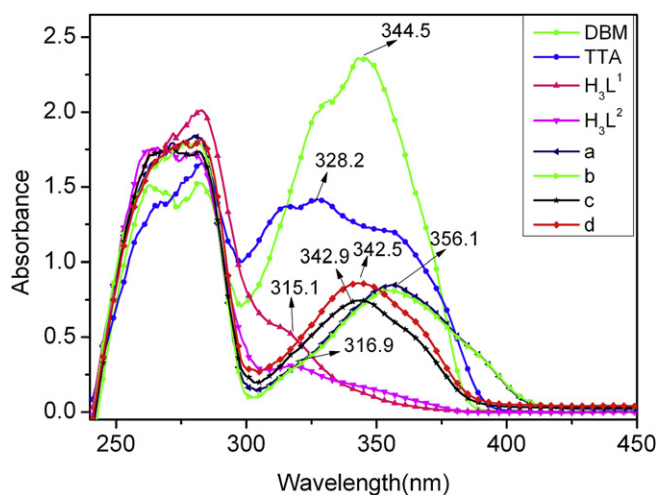


Fig. 4. UV–vis spectra of ligands and trinuclear europium complexes in THF solution (1×10^{-5} mol/L).

in Fig. 4. The UV–vis absorption spectra of complexes (a) and (b) were analogical because the absorption spectra of lanthanide complexes were attributed to the organic ligands and the absorption of lanthanide ions was so weak that can be neglected. For complexes (a) and (b), two main absorption bands at ca. 283 nm and 356 nm were observed, which were attributed to the single–singlet $\pi \rightarrow \pi^*$ enol absorption. For complexes (c) and (d), the main absorption bands were located at ca. 273 nm and 343 nm. Due to the formation of larger conjugated chelate rings in the trinuclear europium complexes, the main absorption bands shifted to longer wavelengths compared with corresponding ligands.

3.5. XRD analysis

The crystallization of europium complexes can lead to diminished device performance of luminescent materials. In order to know the crystalline properties of these trinuclear complexes, the XRD patterns for all complexes were obtained and shown in Fig. S1. In the XRD patterns of these complexes powder in the figures, it was clearly found that some characteristic crystal peaks at 2θ angle of $5\text{--}25^\circ$ for complexes (b), (c) and (d). The complex (a) was amorphous material, which was attributed to the effect of coordinated water molecules in the complex.

3.6. Thermogravimetric analysis (TGA)

The thermal stability of the complexes is very important because the decomposition leads to decrease device performance of europium ion complexes. To investigate the thermal stability of all trinuclear complexes, thermogravimetric analysis (TGA) were carried out at a heating rate of $10^\circ\text{C min}^{-1}$ under a nitrogen atmosphere. Fig. S2 presented the thermogravimetric weight loss curves of all complexes. As seen from the TG curves, the decomposition progress of complexes (b) and (c) were similar. The TG curves were showed that the temperatures of the thermoal decomposition of these two complexes were higher than 250°C , which made device fabrication by vacuum evaporation more feasible. In the first step of decomposition of these complexes a weight loss of about 45% corresponded to loss of ligands TTA and H_3L^1 for complex (c), and ligands DBM and H_3L^2 for complex (b). The second step occurred from 463°C to 610°C for complex (c) (weight loss about 22%), to 593°C for complex (b), which were attributed to the decomposition of phen. The complex (a) had a mass loss (ca. 6%) from 50°C until 100°C , which was attributed to the loss of coordinated and physically water molecules. On further heating, the complex loses weight continuously, the weight loss in the temperature range $100\text{--}421^\circ\text{C}$ amounted to a weight loss of 48%, corresponding to the decomposition of ligands DBM and H_3L^1 . The third weight loss (32%) occurred from 421°C to 633°C , which was attributed to the decomposition of phen. For complex (d), there were two main successive mass loss stages from 50°C to 800°C . The first mass loss stage started at 116°C , ended at 404°C and reached the largest rate at 349°C with mass loss percentage of 68.1%, which was attributed to the mass loss (calculated value 65.9%) of ligands TTA and H_3L^2 . The second stage with about 17.6% mass loss started at 420°C , finished at 670°C and reached the largest rate at 615°C , the mass loss percentage was near the loss of three phen molecules from the complex (calculated value 17.4%). The residual percentage weight (about 14.3%) at the end of the decomposition of the complex was near the mass value (calculated 17.1%) of Eu_2O_3 . These results suggested all trinuclear europium complexes exhibited good thermal properties.

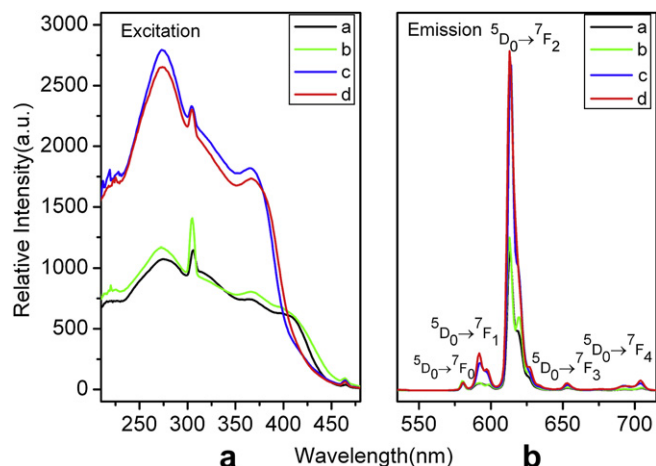


Fig. 5. The PL spectra of trinuclear europium complexes in solid state. (a) Excitation spectra ($\lambda_{em} = 613$ nm for all complexes), (b) Emission spectra ($\lambda_{ex} = 367$ nm for complexes a and b, 364 nm for complexes c and d).

3.7. Photoluminescent properties

3.7.1. Luminescence spectra

β -diketone is already well-known to be a good chelating group to sensitize the luminescence of the europium ion. The mechanism is usually described as the antenna effect: the organic ligands reinforce the energy absorption ability and transfer is to europium ion with high efficiency. Then the characteristic emission from the europium ions excited state will be observed [22].

3.7.2. Fluorescent excitation and emission spectra of the trinuclear europium complexes

The photoluminescent (PL) properties of all trinuclear europium complexes in solid state and solution were investigated in detail at room temperature. The excitation spectra of all complexes in solid and THF solution were obtained by monitoring the $^5D_0 \rightarrow ^7F_2$ transition of europium ion, which were shown in Fig. 5(a) and Fig. 6(a), respectively. For solution excitation spectra, there were two intense board bands at 250–330 nm and 350–425 nm. While in solid state excitation spectra, it can be seen clearly that intense board bands between 250 nm and 425 nm dominate the large portions of excitation spectra of all europium complexes, which were attributed to the $\pi \rightarrow \pi^*$ transitions of ligands (H_3L^1 , H_3L^2 , DBM and TTA)

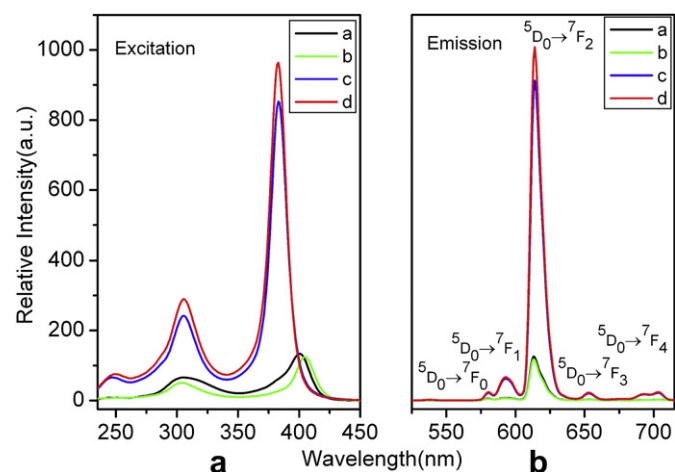


Fig. 6. The PL spectra of trinuclear europium complexes in THF solution (1×10^{-5} L). (a) Excitation spectra ($\lambda_{em} = 613$ nm for all complexes), (b) Emission spectra ($\lambda_{ex} = 404$ nm for complexes a and b, 382 nm for complexes c and d).

from the comparison of the UV–vis spectra in Fig. 4. The excitation spectra of all trinuclear europium complexes in solid state, in addition to the intense broad bands, a weak excitation peak was observed at 463 nm, which result from the $^5D_0 \rightarrow ^7F_1$ transition of europium ion. In comparison with the excitation broad bands of ligands, the direct excitation peaks of europium ion were much weaker. This suggested that emissions of europium by ligands were much more efficient than direct excitation of the trinuclear europium complexes. Meanwhile, the strongly bright red emissions of trinuclear europium complexes in THF solution, upon illuminating with a 365 nm excitation light provided by a 12 w ultraviolet lamp, can be easily observed by the naked eye (Fig. 7).

The mechanism of the energy transfer from ligands to metal ions has been widely discussed to interpret the luminescence of lanthanide compounds [23]. From the results discussed above, we can presume that the energy gaps of the europium ions were comparable with the triplet state energy of the ligands H_3L^1 and H_3L^2 , and then efficient energy transfer can take place from ligands to europium ions. These complexes exhibited characteristic red emission of europium ions by 365 nm excitation and suggested these complexes can be potential red fluorescent materials.

The emission spectra of these complexes in solid state were shown in Fig. 5(b), and characteristic europium ion emissions were observed. The lines were distributed mainly in the 450–700 nm range, which were associated with the $4f \rightarrow 4f$ transitions of the 5D_0 excited state to its low-lying 7F_j ($J = 0, 1, 2, 3$ and 4) levels of europium ions. No emission peaks from the ligands were observed under this excitation, further confirming that the energy transfer from ligands to europium ion center was quite efficient in all trinuclear europium complexes. As well-known, the emissions of

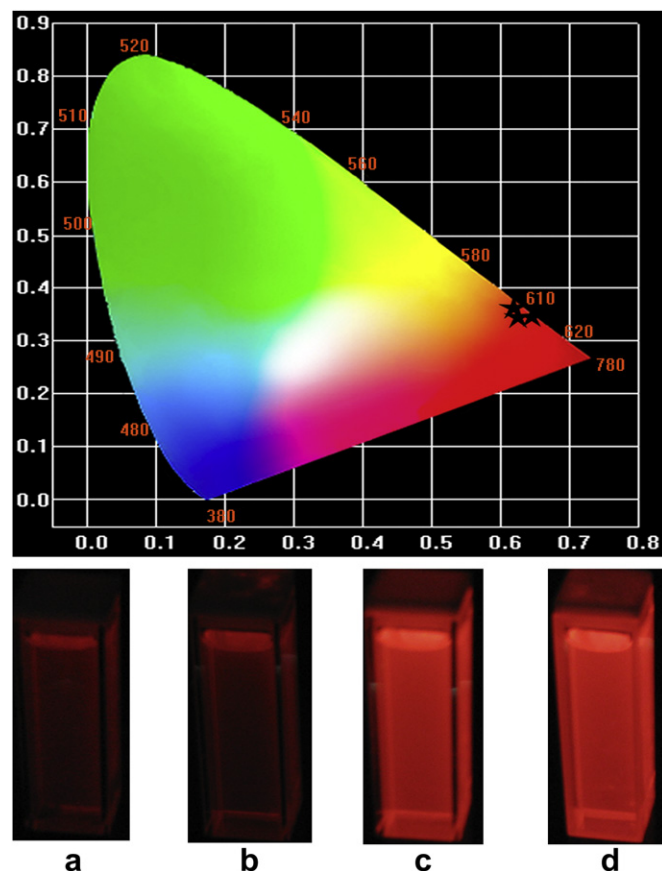


Fig. 7. CIE coordinates diagram of trinuclear europium complexes in solid state and in THF solution.

europium ions were usually employed as a sensitive probe to investigate the coordination and local environment around cations. For europium ion transitions, observed in the emission spectrum, occur via three main mechanisms: forced electric dipole, magnetic dipole, and dynamic coupling. From the emission spectra, we can see the emissions bands at about 580 nm and 653 nm were very weak since their corresponding transitions ${}^5D_0 \rightarrow {}^7F_{0,3}$ were forbidden both in magnetic and electric dipole schemes. A prominent feature that may be noted in these spectra was very high intensity of ${}^5D_0 \rightarrow {}^7F_2$ transition at 613 nm. It was well-known to us that the ${}^5D_0 \rightarrow {}^7F_1$ transition was a parity allowed magnetic dipole (MD) and was nonsensitive to the local structure environment, while the ${}^5D_0 \rightarrow {}^7F_2$ transition was a typical electric dipole (ED) transition and was sensitive to the coordination environment to the europium ion. When the interactions of the rare-earth complex with its local environment were stronger, the complex becomes more nonsymmetrical, and the intensity of the electric-dipolar transitions becomes more intense. As a result, the integration intensity ratio of the ${}^5D_0 \rightarrow {}^7F_2$ transition to ${}^5D_0 \rightarrow {}^7F_1$ transition (I_2/I_1) has been widely used as an indicator of europium ion site symmetry. The calculated results were shown in Table 1.

Whether in solid state or THF solution, the intensity ratios of these trinuclear complexes were very high. In solid state, the intensity ratios (I_2/I_1) of the complexes (a), (b), (c) and (d) were 13.15, 15.02, 9.72, and 8.83, respectively. And in THF solution were 16.33, 16.54, 13.48, and 13.27, respectively. This ratio was only possible when the europium ion did not occupy a site with inversion symmetry. It was clear that strong coordination interactions take place between the organic ligands and europium ion. Further, the emission spectra of the complexes showed only one line for ${}^5D_0 \rightarrow {}^7F_0$ transition, indicating that the presence of a single chemical environment around the europium ions [24,25]. In addition, no emission from the ligands was observed in Fig. 5(b), this indicated that a very efficient energy transfer occurred from the ligands to the central europium ion.

As well-known, for europium ion, the sensitive ability of ligand TTA was better than ligand DBM, so the relative emission intensity of corresponding trinuclear europium complexes based on TTA as ligand were stronger than these complexes based on DBM as ligand under the same conditions. Among these trinuclear europium complexes, the relative luminescent intensity for the corresponding complexes based on H_2L^1 were weaker than these complexes based on H_3L^2 as ligand, it was can be explained by non-radiative deactivation of the energy of excited state as a result of their interaction with high frequency stretching vibrations of C–H groups, because ligand H_3L^1 containing with three methyl groups in center benzene ring [26,27].

In addition to the emission spectra of solid complexes, the room temperature emission spectra of all trinuclear europium complexes in THF solution were investigated (Fig. 6(b)). Compared with the in solid state, no great differences in emission spectra for all complexes in THF solution are observed except no splitting in the ${}^5D_0 \rightarrow {}^7F_1$ and ${}^5D_0 \rightarrow {}^7F_2$ transitions.

Whether in solid or THF solution, the CIE chromaticity coordinates of all trinuclear europium complexes from emission spectra ($\lambda = 365$ nm) were nearly $x = 0.65$ and $y = 0.33$, these results showed pure red color around 100% in the CIE gamut space (Fig. 7). The result was important because it indicated an advantage for rare-earth complexes for preparing OLEDs.

3.7.3. Luminescence decay times (τ) and emission quantum yield

3.7.3.1. In solid state. To better understand the PL properties of trinuclear europium complexes in solid state, the room temperature (RT) luminescence decay curves of the 5D_0 excited state were measured by monitoring the most intense emission lines (${}^5D_0 \rightarrow {}^7F_2$) of europium ion center at 613 nm, and under excitation 325 nm Xenon lamp. As shown in Fig. S3, the decay curves of all complexes exhibited monoexponential behavior, indicative of the presence of a single chemical environment around the europium ion in these complexes, which was in agreement with the results of only one ${}^5D_0 \rightarrow {}^7F_0$ line in the emission spectra. The luminescence time values (τ) of (a), (b), (c) and (d) are 0.36, 0.35, 1.06, and 1.12 ms, respectively. The shorter lifetime of europium ion in complex (c) compared to that of complex (d) may be caused by the quenching of stretching vibrations of C–H group in ligand H_3L^1 .

The intrinsic luminescence quantum yield (Φ_{LN}) of the 5D_0 emission level in these trinuclear europium complexes at room temperature was obtained based on the luminescence data (emission spectra and emission decay curves of these complexes). Eq. (1) a means to determine the Φ_{LN} values from experimental spectroscopic data [28].

$$\Phi_{LN} = \frac{A_{rad}}{A_{rad} + A_{nrad}} \quad (1)$$

Where, A_{rad} and A_{nrad} are radiative and non-radiative transition rates, respectively. The denominator in Eq. (1) is calculated from the lifetime of the emitting level ($1/\tau = A_{rad} + A_{nrad}$). In the case of europium luminescence the value of A_{rad} can be estimated by spectral analysis with the help of Eq. (2) [29].

$$A_{rad} = \frac{A_{0-1} h \omega_{0-1}}{S_{0-1}} \sum_{j=0}^4 \frac{S_{0-j}}{h \omega_{0-j}} \quad (2)$$

Where, J represents the final ${}^7F_{0-6}$ levels, S is the integrated intensity of the particular emission lines and $h\omega$ stands for the corresponding transition energies. A_{0-1} is the Einstein coefficient of spontaneous emission between the 5D_0 and the 7F_1 Stark levels. The branching ratios for the ${}^5D_0 \rightarrow {}^7F_{5,6}$ transitions must be neglected as they are too weak to be observed experimentally. Therefore, their influence can be ignored in the depopulation of the 5D_0 excited state. The ${}^5D_0 \rightarrow {}^7F_1$ transition does not depend on the local ligand field seen by europium ions and, thus, may be used as a reference for the whole spectrum, in vacuo $A_{0-1} = 14.65 \text{ s}^{-1}$ [30]. An average refractive index equal to 1.5 was considered, leading to $A_{0-1} \approx 50 \text{ s}^{-1}$.

Table 1
Solid state and solution luminescent data of trinuclear europium complexes.

Complexes	In solid state								In THF solution	
	τ (ms) ^b	A_{tot} (s ⁻¹)	A_{rad} (s ⁻¹)	A_{nrad} (s ⁻¹)	I_2/I_1 ^c	Φ_{LN} (%)	Q_2 (10 ⁻²⁰ cm ²)	Q_4 (10 ⁻²⁰ cm ²)	I_2/I_1	Φ (%)
a	0.36	2818.5	760.03	2058.3	13.15	26.97	11.3	1.5	16.33	2.97
b	0.35	2877.69	804.31	2073.38	15.02	27.95	12.6	1.3	16.54	3.76
c	1.06	943.4	540.6	402.8	9.72	57.3	16.1	1.6	13.48	30.25
d	1.12	892.86	555.89	336.97	8.83	62.3	18.4	1.8	13.27	32.18
Eu(TTA) ₃ Phen ^a	0.69	1456	698.5	757.5	–	48	26.3	5.7	–	–

^a Those values for Eu(TTA)₃Phen were reported in Ref [32].

^b The integrated intensity ratio of the ${}^5D_0 \rightarrow {}^7F_2$ transition to ${}^5D_0 \rightarrow {}^7F_1$.

^c For ${}^5D_0 \rightarrow {}^7F_2$ transition of europium ions.

According to the above discussion, the intrinsic luminescence quantum yield of these trinuclear europium complexes in solid can be determined, as shown in Table 1.

3.6.4. In THF solution

Solution luminescent yield of the trinuclear europium complexes were determined using quinine sulfate (dissolved in 0.5 M H₂SO₄ with a concentration of 10⁻⁶ M, assuming Φ_{PL} of 0.55) as a standard [31]. The luminescent efficiency was calculated according the following formula:

$$\Phi = \Phi_r \frac{A_r}{A} \cdot \frac{S}{S_r} \cdot \frac{n^2}{n_r^2} \quad (3)$$

Where Φ is the fluorescence quantum yield, S represents the area of the corrected emission fluorescence spectrum, A is the absorbance of the solution at the exciting wavelength, and n is the refractive index of the solvent used. The subscript r denotes the reference substance that its fluorescence quantum yield is already known. The calculated results were shown in Table 1.

Whether in solid state or THF solution, these trinuclear europium complexes exhibited relative high luminescence quantum yield, indicating that the energy transfer from ligands to emitted center europium ions was very efficient. From the Table 1, we found the trinuclear europium complexes based on TTA as another β -diketone ligand exhibited higher luminescence quantum yield than these complexes based on DBM as another β -diketone ligand. This finding was in agreement with the results from luminescent emission intensity. In solid state, the complexes (a) exhibited the lowest luminescent quantum yield (26.97%) in these complexes, which was mainly due to the quenching effect of coordinated water in this complex and the energy loss of C–H oscillator in ligand H₃L¹. Especially, due to the contribution two addition europium ion lumophors, the luminescent quantum yield of trinuclear europium complexes (c) and (d) (57.3% and 62.3%) were higher than that mononuclear europium complex ($\eta = 48\%$) [32]. The result indicated that the introduction of ligands with multiple binding sites in europium complex could effectively increase the quantum yield of europium complexes.

3.7.4. Judd–Ofelt intensity parameters

To investigate the possible structural changes around the emitting center europium ion among these trinuclear complexes, the Judd–Ofelt intensity parameters Ω_2 and Ω_4 (the Ω_6 parameter was not determined because the ⁵D₀→⁷F₆ transition could not be experimentally detected) can be calculated from the emission spectra as the reference [25,33]. In particular, Ω_2 was more sensitive to the symmetry and sequence of ligand fields. To produce faster europium radiation rates, antisymmetrical europium complexes with large Ω_2 parameters need to design. The spontaneous emission probability $A_{0\lambda}$ ($\lambda = 2, 4$) of the transitions were related to its dipole strength according to the equation [25]:

$$A_{0\lambda} = \left(64\pi^4\nu^3\right) / \left|3h(2J+1)\right| \left\langle \left|n(n^2+2)\right| / 9 \left|S_{(ED)} + S_{(MD)}\right| \right\rangle \quad (4)$$

Here, ν is the average transition energy in cm⁻¹, h is Planck constant, $2J+1$ is the degeneracy of the initial state. $S_{(ED)}$ and $S_{(MD)}$ are the electric dipole strength and magnetic dipole strengths, respectively. Among all these transitions, ⁵D₀→⁷F_{0, 3, 5} transitions are forbidden both in magnetic and electric dipole schemes ($S_{(ED)}$ and $S_{(MD)}$ are zero). In addition, ⁵D₀→⁷F₁ transition is the isolated magnetic dipole transition and has no electric dipole contribution, which is practically independent of the lanthanide ions chemical environment and can be used as a reference. The Judd–Ofelt parameters Ω_2 and Ω_4 can be calculated according to the equation [34]:

$$\Omega_\lambda = \frac{3hc^3A_{0-\lambda}}{4e^2w^3\chi \left\langle {}^5D_0 \parallel U^{(\lambda)} \parallel {}^7F_J \right\rangle^2} \quad (5)$$

Where, e is the electronic charge. $\chi = n_0(n_0^2 + 2)^2/9$ is a Lorenz local field correction. The square reduced matrix elements are $\langle {}^5D_0 \parallel U^{(2)} \parallel F_2 \rangle^2 = 0.0032$ and $\langle {}^5D_0 \parallel U^{(4)} \parallel F_4 \rangle^2 = 0.0023$ [35], and an average index of refraction equal to 1.5 was used. The Ω_2 and Ω_4 intensity parameters for all complexes were shown in Table 1. A point to be noted in these results was the relatively high Ω_2 parameter for all complexes. This might be interpreted as being a consequence of the hypersensitive behavior of the ⁵D₀→⁷F₂ transition, indicating that the europium ion was in a highly polarizable chemical environment in these trinuclear complexes.

4. Conclusions

In this work, a series of novel trinuclear europium complexes with tris- β -diketones have been designed, synthesized and characterized by FT-IR, ¹H NMR, ¹³C NMR, ESI-MS, XRD, UV–visible, photoluminescence (PL) spectroscopy, element analysis and thermogravimetric analysis (TGA). Whether in solid state or THF solution, the emission spectra for all complexes displayed the characteristic emission lines for europium ion. The results of decay curves and emission spectrum of trinuclear complexes indicated that there was only one luminescence center, and europium ion was located in a polarized chemical environment. On the basis of the emission spectra and lifetime of the ⁵D₀ emitting level, the intrinsic luminescence quantum yield Φ_{LN} and experimental intensity parameters ($\Omega_{2,4}$) of the ⁵D₀ europium ion excited state were calculated, these results indicated all complexes exhibited relative high Φ_{LN} and Ω_2 . Due to the presence of C–H oscillators in ligand H₃L¹, the Φ_{LN} of the trinuclear europium based on H₃L¹ as ligand were weaker than the complex based on H₃L² as ligand. Further, the trinuclear europium complexes with TTA exhibited much longer lifetime and higher Φ_{LN} than mononuclear europium complex. Especially, due to the contribution of addition two europium lumophors in trinuclear europium complexes, these complexes containing TTA exhibited much longer lifetime and higher intrinsic quantum yield than mononuclear europium complex Eu(TTA)₃phen. The result indicated that the introduction of ligands with multiple binding sites in europium complex could effectively increase the quantum yield of europium complexes. The CIE chromaticity coordinate presented high red color purity 100%. Meanwhile, TGA results showed that all complexes had good thermal stability.

Acknowledgments

This project was supported by Guangdong-Hongkong Technology Cooperation Finding (Project No. 2009A091300012) and the Natural Science Foundation of Guangdong Province of China (Project No.: 8251065004000001 and E06200692).

Appendix. Supplementary data

Supplementary data related to this article can be found online at doi:10.1016/j.dyepig.2011.06.022.

References

- [1] Tang C-W, VanSylke S- A. Organic electroluminescent diodes. Appl Phys Lett 1987;51:913–5.
- [2] Zeng F-H, Ni J, Wang Q-G, Ding Y-B, Ng W-W, Zhu W-H. Structures, and photoluminescence of zinc(II), cadmium(II), and mercury(II) coordination polymers constructed from two novel tetrapyrrolyl ligands. Cryst Growth Des 2010;10:1611–22.

- [3] Wei K-J, Xie Y-S, Ni J, Zhang M, Liu Q-L. Syntheses, crystal structures, and photoluminescent properties of a series of M(II) coordination polymers containing M-X2-M bridges: from 1-D chains to 2-D networks. *Cryst Growth Des* 2006;6:1341–50.
- [4] Liu Z-W, Guan M, Bian Z-Q, Nie D-B, Gong Z-L, Li Z-B, et al. Red phosphorescent iridium complex containing carbazole-functionalized β -diketonate for highly efficient nondoped organic light-emitting diodes. *Adv Funct Mater* 2006;16:1441–8.
- [5] Ho C-L, Wong W-Y, Gao Z-Q, Chen C-H, Cheah K-W, Yao B, et al. Red-light-emitting iridium complexes with hole-transporting 9-arylcarbazole moieties for electrophosphorescence efficiency/color purity trade-off optimization. *Adv Funct Mater* 2008;18:319–31.
- [6] Li B, Li M-T, Hong Z-R, Li W-L, Yu T-Z, Wei H-Z. Observation of red intraligand electrophosphorescence from a stilbene-containing Re(I) complex. *Appl Phys Lett* 2004;85:4786–8.
- [7] Crosby GA, Whan RE, Alire RM. Intramolecular energy transfer in rare earth chelates. Role of the triplet state. *J Chem Phys* 1961;34:743–8.
- [8] Bassett AP, Magennis SW, Glover PB, Lewis DJ, Spencer N, Parsons S, et al. Highly luminescent, triple- and quadruple-stranded, dinuclear Eu, Nd, and Sm(III) lanthanide complexes based on bis-diketonate ligands. *J Am Chem Soc* 2004;126:9413–24.
- [9] Irfanullah M, Iftikhar K. New dinuclear lanthanide(III) complexes based on 6,6,7,7,8,8,8-heptafluoro-2,2-dimethyl-3,5-octanedione and 2,2'-bipyrimidine. *Inorg Chem Commun* 2009;12:296–9.
- [10] Yuan J, Sueda S, Somazawa R, Matsumoto K, Matsumoto K. Structure and luminescence properties of the tetradentate β -diketonate-europium(III) complexes. *Chem Lett* 2003;32:492–3.
- [11] Kim YH, Baek NS, Kim HK. Sensitized emission of luminescent lanthanide complexes based on 4-naphthalen-1-yl-benzoic acid derivatives by a charge-transfer process. *Chemphyschem* 2006;7:213–21.
- [12] Petoud S, Muller G, Moore EG, Xu JD, Sokolnicki J, Riehi JP, et al. Brilliant Sm, Eu, Tb, and Dy chiral lanthanide complexes with strong circularly polarized luminescence. *J Am Chem Soc* 2007;129:77–83.
- [13] Li S-F, Zhong G-Y, Zhu W-H, Li F-Y, Pan J-F, Huang W, et al. Dendritic europium complex as a single dopant for white-light electroluminescent devices. *J Mater Chem* 2005;15:3221–8.
- [14] Dong S, Zhang X-Y, Zhou Y, Jiang J-Z, Bian Y-Z. Perylene diimide-appended mixed (phthalocyaninato)(porphyrinato) europium(III) double-decker complex: synthesis, spectroscopy and electrochemical properties. *Dyes Pigment* 2011;11:99–104.
- [15] Wagner ES, Monica FB, Ricardo OF, Gilberto FS, Severino AJ. New homotrimeric lanthanide complexes: synthesis, characterization and spectroscopy study. *J Phys Chem A* 2010;114:10066–75.
- [16] Du N-Y, Tian R-Y, Peng J-B, Mei Q-B, Lu M-G. Cross-linked Alq₃-containing polymers with improved electroluminescence efficiency used for OLEDs. *Macromol Rapid Commun* 2006;27:412–7.
- [17] Yang C-L, Luo J-X, Ma J-Y, Liang L-Y, Lu M-G. Highly quantum efficiency trinuclear Eu³⁺ complex based on tris-diketonate ligand. *Inorg Chem Commun* 2011;14:61–3.
- [18] Chen B, Luo Y-H, Liang H, Xu J, Guo F-Q, Zhang Y-Z, et al. Optical properties of a tetradentate bis(β -diketonate) europium(III) complex. *Spectrochim Acta Part A* 2008;70:1203–7.
- [19] Luo Y-H, Chen B, Wu W-X, Yu X-W, Yan Q, Zhang Q-J. Judd–Ofelt treatment on luminescence of europium complexes with β -diketonate and bis(β -diketonate). *J Lumin* 2009;129:1309–13.
- [20] van der Made AW, van der Made RH. A convenient procedure for bromomethylation of aromatic compounds. Selective mono-, bis-, or tribromomethylation. *J Org Chem* 1993;58:1262–3.
- [21] Bray DJ, Jolliffe KA, Lindoy LF, McMurtrie JC. Tris- β -diketonates and related keto derivatives for use as building blocks in supramolecular chemistry. *Tetrahedron* 2007;63:1953–8.
- [22] Deacon GB, Phillips RJ. Relationships between the carbon-oxygen stretching frequencies of carboxylato complexes and the type of carboxylate coordination. *Coord Chem Rev* 1980;33:227–50.
- [23] (a) Hasegawa Y, Wada Y, Yanagida S. Strategies for the design of luminescent lanthanide(III) complexes and their photonic applications. *J Photochem Photobiol C* 2004;5:183–202; (b) Bunzli JCG, Piguet C. Taking advantage of luminescent lanthanide ions. *Chem Soc Rev* 2005;34:1048–77.
- [24] Feng R, Jiang F-L, Wu M-Y, Chen L, Yan C-F, Hong M-C. Structures and photoluminescent properties of the lanthanide coordination complexes with hydroxyquinoline carboxylate ligands. *Cryst Growth Des* 2010;10:2306–13.
- [25] Li Y-J, Yan B. Photoactive europium(III) centered mesoporous hybrids with 2-thenoyltrifluoroacetone functionalized SBA-16 and organic polymers. *Dalton Trans* 2010;39:2554–62.
- [26] Beeby A, Clarkson IM, Dickens RS, Faulkner S, Parker D, Royle L, et al. Non-radiative deactivation of the excited states of europium, terbium and ytterbium complexes by proximate energy-matched OH, NH and CH oscillators: an improved luminescence method for establishing solution hydration states. *J Chem Soc Perkin Trans 2*; 1999:493–504.
- [27] Davies GM, Aarons RJ, Motson GR, Jeffery JC, Adams H, Faulkner S, et al. Structural and near-IR photophysical studies on ternary lanthanide complexes containing poly(pyrazolyl)borate and 1,3-diketonate ligands. *Dalton Trans*; 2004:1136–44.
- [28] Balamurugan A, Reddy MLP, Jayakanna M. Single Polymer photosensitizer for Tb³⁺ and Eu³⁺ ions: an approach for white light. *J Phys Chem B* 2009;113:14128–38.
- [29] Ferreira R, Pires P, Castro BD, Sa Ferreira RA, Carlos LD, Pischel U. Zirconium organophosphonates as photoactive and hydrophobic host materials for sensitized luminescence of Eu(III), Tb(III), Sm(III) and Dy(III). *New J Chem* 2004;28:1506–13.
- [30] Werts MHV, Jukes RTF, Verhoeven JW. The emission spectrum and the radiative lifetime of Eu³⁺ in luminescent lanthanide complexes. *Phys Chem Chem Phys* 2002;4:1542–8.
- [31] Melhuish WH. Quantum efficiencies of fluorescence of organic substances: effect of solvent and concentration of the fluorescent solute. *J Phys Chem* 1961;65:229–35.
- [32] Zhao X-H, Huang K-L, Jiao F-P, Liu S-Q, Liu Z-G, Hu S-Q. Synthesis and luminescent properties of complexes of Eu(III) with 2-thienyl trifluoroacetate, terephthalic acid and phenanthroline. *J Phys Chem Solids* 2007;68:1674–80.
- [33] Liang H, Xie F. Fluorescent properties of a dendritic ligand europium complex incorporated in polymethylvinylsiloxane. *Spectrochim Acta Part A* 2010;75:1191–4.
- [34] Teotonio EES, Brito HF, Felinto MCFC, Kodaira CA, Malta OL. Luminescence investigations on Eu(III) thenoyltrifluoroacetate complexes with amide ligands. *J Coord Chem* 2003;56:913–21.
- [35] Kodaira CA, Claudia A, Brito HF, Felinto MCFC. Luminescence investigation of Eu³⁺ ion in the RE₂(WO₄)₃ matrix (RE = La and Gd) produced using the Pechini method. *J Solid State Chem* 2003;171:401–7.